

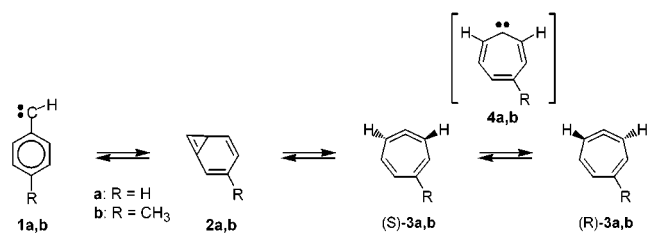
The Enantiomerization Barrier of 5-Methyl-cyclohepta-1,2,4,6-tetraene

Ralf Warmuth

Department of Chemistry, Kansas State University
Manhattan, Kansas 66506

Received March 1, 2001

Arylcarbenes undergo fascinating gas-phase rearrangements.¹ Several aspects related to these rearrangements and the four postulated intermediates **1**–**4** are of great interest: (1) the singlet–triplet gap of **1**,^{2,3} (2) the role of **2** in these rearrangements,^{1d,3} (3) the origin of the different behavior of arylcarbenes and arylnitrenes, which ring-expand in condensed phases contrary to arylcarbenes,^{1c} (4) the enantiomerization of **3** which involves **4** as the transition state structure.³ The nature of the transition state, as well as the influence of the environment on the barrier height, are very important for our understanding of this fundamental step and for the solution-phase chemistry of **3** and **4**.⁴



Recently, we demonstrated that **3a** is stable at room temperature, if protected from bulk phase reactants by incarceration inside a hemicarcerand.^{5–9} Here, we report the inner-phase stabilization of 5-methylcyclohepta-1,2,4,6-tetraene (**3b**) inside the chiral hemicarcerands (*S,S*)-**5** and (*S,S*)-*d*₄₀-**5** and the experimental determination of its enantiomerization barrier, which is the first experimentally measured barrier on an arylcarbene potential energy surface.

We prepared the *p*-tolylcarbene precursor hemicarceplexes (*S,S*)-**5**⊙**7** and (*S,S*)-*d*₄₀-**5**⊙**7** in 31 and 25% yield, respectively

(1) (a) Gaspar, P. P.; Hsu, J.-P.; Chari, S.; Jones, M., Jr. *Tetrahedron* **1985**, *41*, 1479. (b) Johnson, R. P. *Chem. Rev.* **1989**, *89*, 1111. (c) Platz, M. S. *Acc. Chem. Res.* **1995**, *28*, 487. (d) McMahon, R. J.; Abelt, C. J.; Chapman, O. L.; Johnson, J. W.; Kreil, C. L.; LeRoux, J.-P.; Mooring, A. M.; West, P. R. *J. Am. Chem. Soc.* **1987**, *109*, 2459. (e) Bonvallet, P. A.; McMahon, R. J. *J. Am. Chem. Soc.* **1999**, *121*, 10496.

(2) (a) Admasu, A.; Gudmundsdóttir, A. D.; Platz, M. S. *J. Phys. Chem. A* **1997**, *101*, 3832. (b) Seburg, R. A.; Hill, B. T.; Squires, R. R. *J. Chem. Soc., Perkin Trans. 2* **1999**, 2249. (c) Geise, C. M.; Hadad, C. M. *J. Org. Chem.* **2000**, *65*, 8348.

(3) (a) Matzinger, S.; Bally, T.; Patterson, E. V.; McMahon, R. J. *J. Am. Chem. Soc.* **1996**, *118*, 1535. (b) Wong, M. W.; Wentrup, C. *J. Org. Chem.* **1996**, *61*, 7022. (c) Schreiner, P. R.; Karney, W. L.; Schleyer, P. v. R.; Borden, W. T.; Hamilton, T. P.; Schaefer, H. F., III. *J. Org. Chem.* **1996**, *61*, 7030. (d) Patterson, E. V.; McMahon, R. J. *J. Org. Chem.* **1997**, *62*, 4398.

(4) (a) Harris, J. W.; Jones, W. M. *J. Am. Chem. Soc.* **1982**, *104*, 7329. (b) Kirmse, W.; Loosen, K.; Sluma, H.-D. *J. Am. Chem. Soc.* **1981**, *103*, 5935. (c) Kirmse, W.; Sluma, H.-D. *J. Org. Chem.* **1988**, *53*, 763.

(5) (a) Warmuth, R.; Marvel, M. A. *Angew. Chem.* **2000**, *112*, 1168; *Angew. Chem., Int. Ed.* **2000**, *39*, 1117. (b) Warmuth, R.; Marvel, M. A. *Chem. Eur. J.* **2001**, *7*, 1209. (c) Warmuth, R. *Eur. J. Org. Chem.* **2001**, 423.

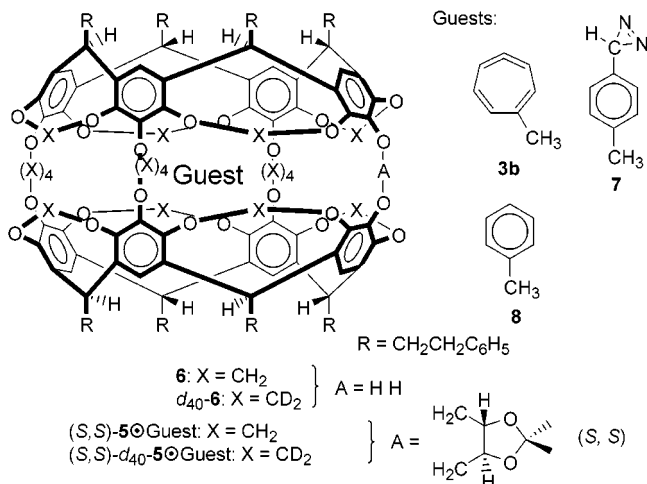
(6) (a) Cram, D. J.; Cram, J. M. *Container Molecules and Their Guests*; Stoddart, J. F., Series Ed.; The Royal Society of Chemistry: Cambridge, U.K. 1994; p 131. (b) Jasat, A.; Sherman, J. C. *Chem. Rev.* **1999**, *99*, 931. (c) Yoon, J.; Warmuth, R. *Acc. Chem. Res.* **2001**, *34*, 95.

(7) Warmuth, R. *Inclusion. Phenom.* **2000**, *37*, 1.

(8) Cram, D. J.; Tanner, M. E.; Thomas, R. *Angew. Chem.* **1991**, *103*, 1048; *Angew. Chem., Int. Ed. Engl.* **1991**, *30*, 1024.

(9) (a) Warmuth, R. *Angew. Chem.* **1997**, *109*, 1406; *Angew. Chem., Int. Ed. Engl.* **1997**, *36*, 1347. (b) Warmuth, R. *J. Chem. Soc., Chem. Commun.* **1998**, 59.

Chart 1



by reacting **6**¹⁰ or *d*₄₀-**6** with (*S,S*)-(-)-1,4-di-*O*-tosyl-2,3-*O*-isopropylidene-*L*-threitol and Cs₂CO₃ in HMPA in the presence of excess **7** (Chart 1). The room temperature ¹H NMR spectrum of a degassed solution of (*S,S*)-*d*₄₀-**5**⊙**7** or of (*S,S*)-**5**⊙**7** in *d*₈-toluene, which had been extensively irradiated ($\lambda > 320$ nm, 77 K), showed two new hemicarceplexes (47 and 32% overall yield, respectively), which are formed in a 1:1.8 ratio together with unidentified innermolecular insertion products. We assign both hemicarceplexes to the diastereomers (*S,S*)-*d*₄₀-**5**⊙(+)-**3b** and (*S,S*)-*d*₄₀-**5**⊙(-)-**3b**. Our assignment is based on the known matrix photochemistry of *p*-tolylcarbene,¹¹ and on the reaction of the guest **3b** with oxygen leading to CO₂ and the toluene hemicarceplex (*S,S*)-*d*₄₀-**5**⊙**8** (Figure 1d).^{5a,b} In the ¹H NMR spectrum of incarcerated **3b**, the singlets assigned to the methyl protons of both enantiomeric guests appear upfield shifted at $\delta -1.47$ and -1.57 (Figure 1c). Above 98 °C both singlets broaden as compared to other singlets of innermolecular *p*-tolylcarbene insertion products. We interpret this line broadening with a dynamic exchange between (*S,S*)-*d*₄₀-**5**⊙(+)-**3b** and (*S,S*)-*d*₄₀-**5**⊙(-)-**3b** via the guest enantiomerization. A line shape analysis provided the exchange rate constants, k_{+1} and k_{-1} , between 98 and 115 °C.

We further extended the temperature range via chemical relaxation experiments. Thus, photolysis of a degassed solution of (*S,S*)-*d*₄₀-**5**⊙**7** in *d*₈-toluene as described above and slow warm-up of this sample from 77 to 248 K in the NMR spectrometer probe yielded a diastereomeric ratio of 1:1.15 (Figure 1b). This ratio remained constant over the course of 1 h. At 263 K, the perturbed system slowly relaxed to the thermodynamic diastereomeric ratio of 1:1.9 with a relaxation rate constant $k_{\text{relax}} = 1.6 \pm 0.2$ s⁻¹. The latter is the sum of the enantiomerization rate of the minor $k_{+1} = 1.0$ s⁻¹ and of the major diastereomer $k_{-1} = 0.6$ s⁻¹.

Arrhenius plots provided activation energies, pre-exponential factors and free energies of activation for the enantiomerization of the minor enantiomer $E_a(\text{minor}) = 19.6 \pm 0.2$ kcal/mol, $\log A(\text{minor}) = 12.2 \pm 0.2$, and $\Delta G^\ddagger_{298}(\text{minor}) = 19.1 \pm 0.3$ kcal/mol and $E_a(\text{major}) = 20.3 \pm 0.2$ kcal/mol, $\log A(\text{major}) = 12.3 \pm 0.2$, and $\Delta G^\ddagger_{298}(\text{major}) = 19.4 \pm 0.3$ kcal/mol for the major enantiomer (Figure 2).¹² These measured barriers are in excellent

(10) (a) Kurdistani, S. K.; Helgeson, R. C.; Cram, D. J. *J. Am. Chem. Soc.* **1995**, *117*, 1659. (b) Yoon, J.; Sheu, C.; Houk, K. N.; Knobler, C. B.; Cram, D. J. *J. Org. Chem.* **1996**, *61*, 9323.

(11) West, P. R.; Mooring, A. M.; McMahon, R. J.; Chapman, O. L. *J. Org. Chem.* **1986**, *51*, 1316.

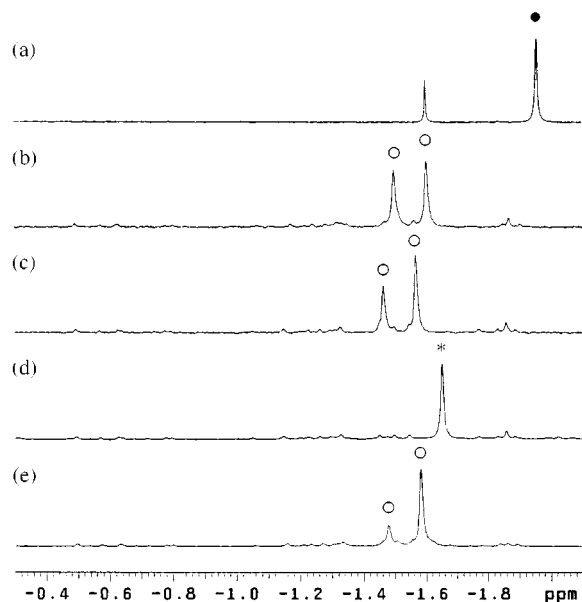


Figure 1. Partial ^1H NMR spectra of (S,S) - $(+)$ - d_{40} - $5\text{O}7$ (d_8 -toluene, 400 MHz) before (a) and after (b–e) extensive photolysis at 77 K. (b) Recorded at 248 K immediately after the photolysis; (c) sample (b) recorded at 263 K after 3 h at 263 K; (d) sample (c) after exposure to oxygen; (e) spectrum recorded at 258 K after a freshly photolyzed sample had been 8 weeks at 77 K. Singlets assigned to the methyl protons of **3b**, **7**, and **8** are marked with an open circle, a black dot, and an asterisk, respectively.

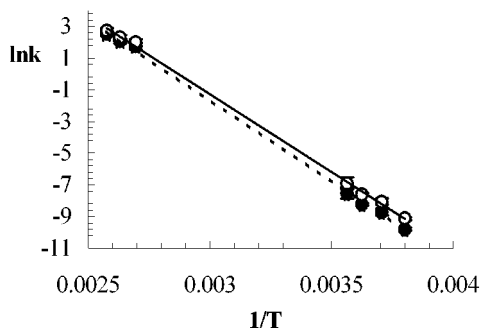


Figure 2. Arrhenius plots for the enantiomerization of the minor diastereomeric hemicarceplex (S,S) - d_{40} - $5\text{O}3\text{b}$ (\square ; —) and the major diastereomeric hemicarceplex (S,S) - d_{40} - $5\text{O}3\text{b}$ (\bullet ; - - -).

agreement with results of DFT calculations (B3LYP/6-311G**), which predict $\Delta E = 21.1$ kcal/mol and $\Delta G_{298} = 20.0$ kcal/mol for the energy difference between **3b** and closed-shell $^1\text{A}_1$ -**4b**, even though the DFT method is known to overestimate the stability of allenes.^{3d,13}

A surprising observation was made, when a photolyzed solution was left in the dark at 77 K for several weeks and then warmed to 258 K. The ^1H NMR spectrum showed a diastereomeric ratio of 1:3.5, which strongly differed from that measured immediately after the photolysis (Figure 1e). Upon further warming, this ratio changed to the thermodynamic ratio of 1:1.9. Although the exact

mechanism of the diastereomeric ratio change at 77 K is not fully understood, it could either result from low-temperature equilibration via a tunneling mechanism, or from a selective decomposition reaction of the minor isomer at 77 K. For example, if both diastereomeric hemicarceplexes are exposed to oxygen at 263 K, the minor enantiomer reacts 2.5 times faster than the major enantiomer to yield (S,S) - d_{40} - $5\text{O}8$ as a consequence of the host-induced destabilization of the faster reacting guest. ($k_{\text{major}} = 3.9 \pm 0.1 \cdot 10^{-4} \text{ s}^{-1}$; $k_{\text{minor}} = 1.00 \pm 0.04 \cdot 10^{-3} \text{ s}^{-1}$).

Several important conclusions can be drawn from our experiments. (1) From the average enantiomerization barrier $E_a(\mathbf{3b}) = 20.0 \pm 0.3$ kcal/mol, we estimated the barrier for **3a**.

Recently, we determined a lower limit of $\Delta G_{373}^\ddagger(\mathbf{3a}) > 19.6$ kcal/mol based on the absence of dynamic line broadening in the high temperature ^1H NMR spectrum of (S,S) - $5\text{O}3\text{a}$ ($R = \text{pentyl}$).^{5b} For **3b**, we expect a lower enantiomerization barrier by about 1–1.5 kcal/mol due to the methyl substituent, which stabilizes **4b** better as compared to **3b**. This predicted stabilization of **4b** is similar to the effect of the *p*-methyl group on the singlet–triplet gap of *p*-tolylcarbene as compared to phenylcarbene.^{2c} Thus, a good estimate is $E_a(\mathbf{3a}) = 21.2 \pm 0.4$ kcal/mol. This estimate agrees very well with DFT calculations,^{3a–c} which assume $^1\text{A}_1$ -**4a** as the transition state and with results of CASSCF and CASPT2N calculations assuming $^1\text{A}_2$ -**4a** as the transition-state structure.^{3c} CCSD and MP2 calculations slightly under- or overestimate the experimental barrier.^{3a,b} Uncertain is the influence of the reaction environment (inner phase or gas phase) on these barriers. This might explain the deviation between our estimate and the results of the highest level CCSD calculations. The experimental determination of other barriers on the tolylcarbene potential energy surface will further strengthen this first evaluation of recent ab initio calculations. We are working in this direction. (2) The thermodynamic ratio (S,S) - d_{40} - $5\text{O}(+)$ -**3b**/ (S,S) - d_{40} - $5\text{O}(-)$ -**3b** is much larger than the kinetic ratio or thermodynamic ratio of other diastereomeric hemicarceplexes (S,S) - $5\text{O}(+)$ -Guest/ (S,S) - $5\text{O}(-)$ -Guest.¹⁴ We explain this with the extent of complementarity between inner phase and guest. The inner phase of (S,S) -**5** is spherically shaped and twisted. Likewise is the shape of **3b**. The opposite twist of both enantiomeric **3b** results in very different host–guest interactions in both diastereomeric hemicarceplexes. On the other hand, the shapes of the two early enantiomeric transition states for the ring-expansion of **1b** differ less and will lead to similar host–guest interactions in both diastereomeric transition state hemicarceplexes. Although the diastereomeric excess $de = 7\%$ was modest in the presented example, maximal asymmetric induction in inner-phase reactions can be expected for slightly exothermic reactions with spherical and twisted transition states.

Acknowledgment. I warmly thank the Petroleum Research Fund administered by the American Chemical Society for generous financial support.

Supporting Information Available: Experimental procedures and characterization of new compounds, ^1H NMR spectra of (S,S) - d_{40} - $5\text{O}7$, (S,S) - $5\text{O}7$ and of photolyzed (S,S) - d_{40} - $5\text{O}7$ before and after exposure to oxygen, and line shape analysis of high temperature ^1H NMR spectra (PDF). This material is available free of charge via the Internet at <http://pubs.acs.org>.

JA015743E

(12) Standard errors were estimated by linear least-squares regression of Arrhenius plots; Bevington, P. R.; Robinson, D. K. *Data Reduction and Error Analysis for the Physical Sciences*; 2nd ed.; McGraw-Hill: New York, 1992; Chapter 6.

(13) Plattner, D. A.; Houk, K. N. *J. Am. Chem. Soc.* **1995**, *117*, 4405.

(14) Yoon, J.; Cram, D. J. *J. Am. Chem. Soc.* **1997**, *119*, 11796.